New generation phase coronagraphy

Dimitri Mawet[1], Pierre Riaud[1], Jacques Baudrand[2], Anthony Boccaletti[2], Pierre Baudoz[2] & Jean Surdej[1]

[1] *Institut d'Astrophysique et de Géophysique, Université de Liège, Belgium*
[2] *LESIA, Observatoire de Paris-Meudon, France*
E-mail : mawet@astro.ulg.ac.be

I. Introduction

Phase mask coronagraphy is a technique aiming at accommodating both high dynamic and high angular resolution imaging of faint sources around bright objects (for the optical scheme, see Fig. 1). In the framework of the VLT-Planet Finder/SPHERE developments, we present two novel methods for achromatizing the Four Quadrant Phase Mask coronagraph (FQPM, [1-3]), and a **new phase mask coronagraph** implemented with optimized space-variant **subwavelength** surface-relief **gratings** inducing a second order optical vortex: the Annular Groove Phase Mask (**AGPM**) coronagraph is **fully symmetric** and **free from any "shaded zones"**.

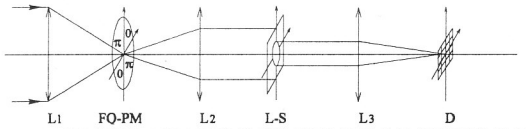

Fig. 1 Common coronagraphic optical scheme shown here in the FQPM case: L1, L2 and L3 are three lenses in the optical system. L1 provides a large *f/d* ratio on the coronagraph; L2 images the pupil in the second plane. The Lyot Stop (L-S) suppresses the diffracted starlight, and finally L3 forms the coronagraphic image on the detector D.

II. Achromatic FQPM with halfwave plates: white light laboratory results

We recently reported [3] laboratory results on white light tests of a FQPM implemented with achromatic Quartz-MgF_2 waveplates: a contrast of 10^{-4} was obtained at 2.5 λ/d between 500 and 900 nm (see Fig. 3). Despite the difficulty of cutting, polishing and assembling the different plates into a FQPM (Fig. 2), these results led us to consider this technique for the VLT-Planet Finder/SPHERE wideband achromatic coronagraph. In this work, we have indeed demonstrated the feasibility of the FQPM coronagraph achromatization by means of birefringent elements, paving the way toward more complex solution involving subwavelength gratings. The halfwave plates (HWP) technique was proved more convenient both to manufacture and to implement than the dispersive achromatization such as the dispersive plate concept. This conclusion comes directly from the fact that the fundamental constraint on the thickness control is relaxed by a factor comparable to the ratio between material indices and birefringences (often 10^{-2}). On the other hand, birefringences must be known at a very good precision as well as their variations with temperature (Fig. 3).

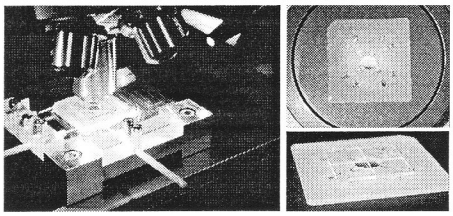

Fig. 2 The achromatic phase mask assembly is mounted on a silica substrate 1mm thick with a central hole of 8mm in diameter. The four Quartz plates are assembled on one side and the four remaining MgF2 plates on the other one. The π phase shift between adjacent quadrants is provided by rotating the fast axis of two quadrant stacks along one diagonal by 90 degrees around their normals. Each of the 8 individual plates is polished (λ/10 PTV at 550 nm) and cut parallel to the optical axis with a micrometric precision. The edge parallelism cutting error with respect to each plate fast/slow axis is below 30 arcsecs. All plates are anti-reflection coated for the considered bandwidth (reflectivity <1%). We then assembled the eight plates with a high precision (<10 µm) while respecting orientations, alignments and coplanarity (<10 arcmin) for the two stages. This task revealed to be practically difficult and long to achieve within the specifications.

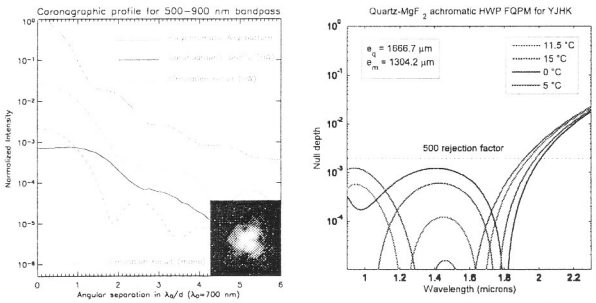

Fig. 3 Left: experimental and theoretical coronagraphic profiles: the grey solid curve is the experimental PSF for the 500–900 nm bandpass. The total exposure time for the PSF is 60 s. The continuous black line shows the coronagrapic profile obtained with our achromatic waveplate mask. The dashed line presents the coronagraphic simulation results taking into account the waveplate phase residuals, the defocus error, the spectral response of the halogen lamp and the camera. For comparison, the dotted line presents the simulation results for a monochromatic mask used in the same conditions. Bottom right: theoretical performance (global null depth) and temperature sensitivity for the optimized YJHK halfwave plate FQPM concept for SPHERE.

III. Subwavelength Gratings / ZOGs

When **the period of the grating is smaller than the wavelength** of the incident light, it does not diffract as a classical spectroscopic grating. All the incident energy is enforced to propagate only in the zeroth order, leaving incident wavefronts free from any further aberrations. Subwavelength gratings are therefore often called Zeroth Order Gratings (ZOGs). This type of gratings behaves like homogeneous media with unique characteristics (e.g. artificial anisotropy). The key point is that by carefully **controlling the grating geometry** (via the grating parameters, see Fig. 4), one may adjust the optical refractive properties. To be more precise, the structure's form birefringence can be tuned in order to induce an achromatic phase shift between the polarization components TE and TM [2].

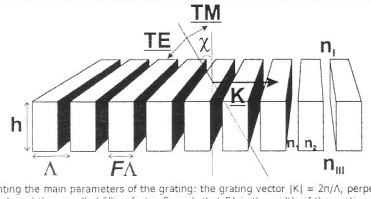

Fig. 4 ZOG schematic presenting the main parameters of the grating: the grating vector |K| = 2π/Λ, perpendicular to the grating lines, with Λ the period, the grating depth h and the so-called filling factor F, such that FΛ is the width of the grating ridges. TE and TM are the vectorial orthogonal polarization components of the X-incident light. n_I and n_{III} are the refractive indices of the incident and transmitting media, respectively. n_1 and n_2 are the refractive indices of the grating itself (in our case, $n_1 = n_I$ and $n_2 = n_{III}$).

Detection and characterization of exoplanets:
Observational challenges for the next decade
Geneva, 28-30 June 2006

IV. ZOGs as Achromatic Phase Shifters

The ZOG design procedure consists in **optimizing the π phase shift quality within a given spectral range for a well-chosen material**. It also requires the equalization of the interfering fluxes, which is difficult to achieve. The merit function to be minimized is the **null depth N(λ)**. The latter measures the darkness of the destructive interference taking place in the pupil plane following the phase mask coronagraph focal plane and is directly related to the phase shift error with respect to π, $\varepsilon(\lambda)$ and the flux ratio $q(\lambda)$

$$N(\lambda) = \frac{\left(1-\sqrt{q(\lambda)}\right)^2 + \varepsilon(\lambda)^2\sqrt{q(\lambda)}}{\left(1+\sqrt{q(\lambda)}\right)^2}$$

A well adapted structure consists in a rectangular profile grating covered with an AR layer [2]. The ZOG solution can accommodate **a large variety of materials** and **wavelength ranges** but we have focussed on Diamond, *ZnSe* and *Si* ZOGs for the H and K bands. RCWA [3] results are displayed in Fig. 5, showing excellent **null depths around 10^{-5} for individual filters and better than 10^{-3} for both of them simultaneously**.

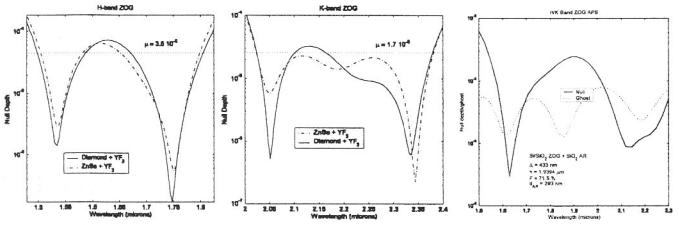

Fig. 5 H/K-band ZOG null depths (logarithmic scale) versus wavelength. Left (H) and middle (K): the continuous curve is for the Diamond YF_3 AR coated ZOG. The dashed curve, for the *ZnSe* YF_3 AR coated one. Right: Silicon SiO_2 AR coated ZOG for H and K bands.

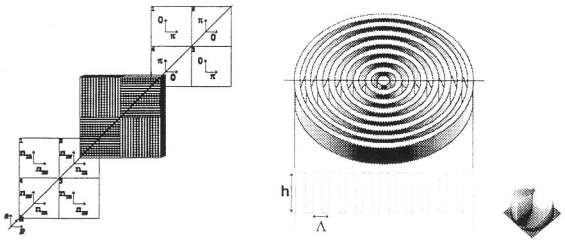

Fig. 6 Left: FQ-PM anti-symmetrical implementation of ZOGs: 4QZOG. Right: concentric space-variant implementation of ZOGs: AGPM.

V. Coronagraphic Implementation

4QZOG: the four gratings engraved on a unique substrate are strictly identical and implemented in the following way: two of them in two quadrants along one diagonal are rotated by 90 degrees around their normals with respect to the two others. This anti-symmetrical configuration achieves the FQ-PM particular focal plane π-phase distribution (Fig. 6).

AGPM: The idea of the AGPM coronagraph was to suppress the "shaded zones" resulting for the quadrant transitions of the 4QZOG. The concentric grooves of the AGPM coronagraph are in fact what is called a **space-variant** subwavelength grating (Fig. 6). At the center of the components, the phase possesses a screw dislocation inducing a phase singularity, i.e. an **optical vortex**. The central singularity forces the intensity to vanish by a total destructive interference, creating a dark core. Whether a dark core is created in the pupil or focal plane of a telescope will determine the way it further evolves. In this poster, we propose to place the optical vortex in the focal plane, filter in the relayed pupil plane and make the detection in a final image plane [5]. This solution is much more attractive (infinite rejection, achromaticity) than a monochromatic pupil plane vortex [6].

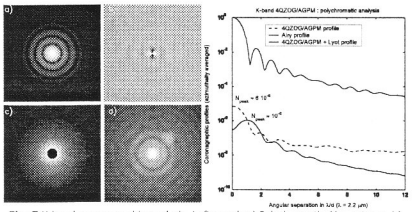

Fig. 7 K-band coronagraphic analysis. Left panel: a) Polychromatic Airy pattern, b) focal plane phase visualisation (after the AGPM), c) relayed pupil plane, where we notice the perfect symmetry of the rejection in an annular way, d) final coronagraphic image revealing the **15 mag fainter** simulated companion. All images are displayed in non linear scale. Right: Coronagraphic profile of the 4QZOG and AGPM.

Table 1. 3-stage modelling results (1- RCWA stage where the form birefringence of the local grating is calculated, 2- Analytical treatment giving the spatial distribution of the output polarization field, 3- Scalar far-field propagation Fourier coronagraphic code with assumed **wavefront qualities of λ/70 rms at 632.8 nm**).

Filters	H (R=4.7)	K (R=5.5)	H/K (R=2)
Null Depth (global)	3.5×10^{-5}	1.7×10^{-5}	1×10^{-3}
Contrast at 3λ/d	2.9×10^{-7}	1.4×10^{-7}	1×10^{-5}
Grating period	500 nm	700 nm	400 nm

VI. Conclusions and prototyping prospects

In this poster, we have presented two novel achromatization methods for the FQPM coronagraph: the halfwave plate technique and the subwavelength grating technology. We have also introduced a brand new phase mask coronagraph: the Annular Groove Phase Mask is inherently quasi achromatic thanks to the use of optimized ZOGs and also suppresses the "shaded zones" of the FQPM allowing a full discovery space and the absence of artefacts in extended object imaging (e.g. circumstellar disks). The two techniques appear complementary since the HWP-FQPM concept offers extremely wideband capabilities (R_c=2) at the cost of stability (delicate bulky mounting, temperature sensitivity,...) and discovery space (FQPM dead zones at the transition) while the subwavelength grating solution is an integrated one (very compact, lightweight and stable) offering valuable performances (Table 1) and provides the possibility of manufacturing the AGPM, alleviating one of the most annoying Achilles'heel of the FQPM coronagraph (Fig. 7). These considerations has led us to consider the manufacturing of Silicon-based 4QZOG and AGPM prototype in collaboration with CEA-LETI and LAOG while pursuing the developments of the HWP-FQPM coronagraph in parallel.

References

[1] Rouan et al. 2000, *PASP* **112**, 1479

[2] Mawet et al. 2005, *Appl. Opt.* **44**, 7313

[3] Mawet et al. 2006, *A&A* **448**, 801

[4] Moharam & Gaylord 1982, *JOSA* **71**, 811

[5] Mawet et al. 2005, *ApJ* **613**, 1191

[6] G.A.Jr. Swartzlander 2001, *OL* **8**(26), 497